Geophysical Research Letters

RESEARCH LETTER
10.1029/2025GL114642

Key Points:

- Clear skies and low water tables caused an Amazonian peatland to switch from a large carbon sink to being carbon neutral
- Canopy photosynthesis was subject to photoinhibition when there were prolonged periods with clear skies and higher solar irradiance
- When the water table dropped below the surface, ecosystem respiration increased

Supporting Information:

Supporting Information may be found in the online version of this article.

Correspondence to:
J. D. Wood and T. J. Griffis,
woodjd@missouri.edu;
timgriffis@umn.edu

Citation:
Wood, J. D., Roman, D. T., Griffis, T. J., Cadillo-Quiroz, H., Del Castillo, D., Fachin, L., et al. (2025). A large Amazonian peatland carbon sink was eliminated by photoinhibition of photosynthesis and amplified ecosystem respiration. *Geophysical Research Letters*, *52*, e2025GL114642. https://doi.org/10.1029/2025GL114642

Received 6 JAN 2025
Accepted 1 MAY 2025

Author Contributions:
Conceptualization: Jeffrey D. Wood, D. Tyler Roman, Timothy J. Griffis
Data curation: D. Tyler Roman
Formal analysis: Jeffrey D. Wood
Funding acquisition: Jeffrey D. Wood, Timothy J. Griffis, Hinsby Cadillo-Quiroz, Lizardo Fachin, Erik Lilleskov, Randall K. Kolka
Investigation: Lizardo Fachin, Jhon Rengifo
Project administration: D. Tyler Roman, Timothy J. Griffis, Lizardo Fachin
Resources: Dennis Del Castillo

A Large Amazonian Peatland Carbon Sink Was Eliminated by Photoinhibition of Photosynthesis and Amplified Ecosystem Respiration

Jeffrey D. Wood[1], **D. Tyler Roman**[2], **Timothy J. Griffis**[3], **Hinsby Cadillo-Quiroz**[4], **Dennis Del Castillo**[5], **Lizardo Fachin**[5], **Erik Lilleskov**[6], **Randall K. Kolka**[7], **Jhon Rengifo**[5], **and Craig Wayson**[2]

[1]School of Natural Resources, University of Missouri, Columbia, MO, USA, [2]USDA Forest Service, International Programs, Washington, DC, USA, [3]Department of Soil, Water, and Climate, University of Minnesota, Saint Paul, MN, USA, [4]School of Life Sciences, Arizona State University, Tempe, AZ, USA, [5]Instituto de Investigaciones de la Amazonia Peruana, Iquitos, Peru, [6]USDA Forest Service, Northern Research Station, Houghton, MI, USA, [7]USDA Forest Service, Northern Research Station, Grand Rapids, MN, USA

Abstract The fate of tropical peatland carbon cycling under environmental change is highly uncertain. We found that a palm swamp peatland in the Peruvian Amazon that was a strong annual sink for 2 years switched to carbon neutral in the absence of a major anthropogenic disturbance. We attributed the change in carbon sink strength to (a) photoinhibition of canopy photosynthesis when skies were clearer and thus solar irradiance higher and (b) increased ecosystem respiration when the water table position was below the peat surface, and heterotrophic respiration was amplified. These mechanisms were not, however, synchronous in time. The importance of photoinhibition as a driver of changes in peatland carbon budgets is a novel finding, and an understudied mechanism of canopy photosynthetic impairment. Shifts in climate that increase periods with sustained high solar irradiance and/or low water table are thus likely to amplify interannual variability in the carbon sink strength.

Plain Language Summary Peatlands store about one third of global soil carbon despite occupying less than 5% of the land area. Recent estimates show that tropical peatlands store much more carbon than previously thought. There are considerable gaps in knowledge regarding the interannual variability of carbon budgets in tropical peatlands and the way that changing environmental conditions influence the carbon cycling in these ecosystems. We show that a palm swamp peatland in the Peruvian Amazon is sensitive to changes in environmental conditions and can flip from a large carbon sink to carbon neutral when there are prolonged periods with (a) clear skies and higher light intensities that impair canopy photosynthesis and (b) a lower water table that increases peat decomposition. These findings show that the carbon budgets of these ecosystems are highly sensitive to environmental variability.

1. Introduction

Peatlands cover 3%–4% of Earth's land surface yet store about one third of global soil carbon (C), making them "keystone ecosystems" in the global C cycle (UNEP, 2022; Z. Yu et al., 2011). The rapid release of C accumulated over thousands of years represents an important, yet highly uncertain, positive feedback on the climate system (Hanson et al., 2020; Z. C. Yu, 2012; Z. Yu et al., 2011). We are particularly interested in tropical peatlands because recent estimates of C stocks of 152–288 Gt-C are significantly higher than previously thought (Ribeiro et al., 2020).

The total peatland area within the Amazon basin is 251,015 km^2 (95% confidence interval [CI], 128,671–373,359), of which 55,890 (28,748–83,032) is in Peru (Hastie et al., 2024). Peruvian peatlands, which occupy about 5% of the total land area, have a belowground C stock of is 5.4 (2.6–10.6) Pg-C, approximately equal to the entire aboveground C stock of Peru (Hastie et al., 2022). Here, we specifically focus on a moriche palm (Mauritia flexuosa L.f) swamp peatland, known locally as aguajales, and are the dominant kind of Amazonian peatland (López Gonzales et al., 2020).

The scant ecosystem flux literature on tropical peatlands has documented substantial interannual variability, with coefficients of variation of annual net ecosystem CO$_2$ exchange (NEE) ranging from 1% to 117% (Table S1 in

Supervision: Lizardo Fachin
Visualization: Jeffrey D. Wood
Writing – original draft: Jeffrey D. Wood
Writing – review & editing: Jeffrey D. Wood, D. Tyler Roman, Timothy J. Griffis, Hinsby Cadillo-Quiroz, Lizardo Fachin, Erik Lilleskov, Randall K. Kolka, Jhon Rengifo

Supporting Information S1) (Deshmukh et al., 2021; Griffis et al., 2020; Hirano et al., 2007, 2012; Kiew et al., 2018, 2020; Ohkubo et al., 2021; Tang et al., 2020). Furthermore, the variability was such that Indonesian peatlands in an intact peat swamp forest (Hirano et al., 2012) and a drained peatland in years after a fire disturbance (Ohkubo et al., 2021) switched from being a CO_2 sink to a source.

Large increases in soil respiration induced when the water table falls below the surface and a peat layer becomes oxic is a classic peatland disturbance response (Hirano et al., 2012; Kiew et al., 2018; Ma et al., 2022). Indeed, tropical peatlands became strong CO_2 sources in response to disturbances that lowered the water table and decreased aboveground biomass, which amplified respiration in the peat, and decreased canopy photosynthesis, respectively (Deshmukh et al., 2021; Hirano et al., 2012; Ohkubo et al., 2021). Tropical peatland hydrology can also be affected by large-scale modes of climate variability like the El Niño-Southern Oscillation, a key factor that regulates peatland C cycling in Southeast Asia (Deshmukh et al., 2021; Hirano et al., 2012; Kiew et al., 2018; Ohkubo et al., 2021). The increase of ecosystem-level CO_2 emissions in response to conditions that lower water tables are often attributed to amplified soil respiration (Deshmukh et al., 2021; Hirano et al., 2012; Kiew et al., 2018). There have, however, been few observations in South American peatlands.

Our previous work at a peatland in Quistococha Peru, found that seasonal variations of NEE were linked to decreased canopy photosynthesis and increased ecosystem respiration during the drier season when the water table was below the surface, but both years were strong annual CO_2 sinks (Griffis et al., 2020). Here, we extend our analyses to include a year when the forest was CO_2 neutral. Though the system experienced a water table drawdown confined to the drier season, it could not explain the dramatic change in the annual net CO_2 budget from sink to neutrality. We tested two hypotheses to diagnose the mechanisms underlying the significant change in the annual net CO_2 budget:

- *Respiration Hypothesis*: When the water table is below the surface, increased soil respiration is triggered, thereby increasing ecosystem respiration, which drastically decreases the net CO_2 sink strength.
- *Photoinhibition of Photosynthesis Hypothesis*: Under clearer skies with high light, photoinhibition decreases canopy photosynthesis and thus the net CO_2 sink strength.

2. Materials and Methods

2.1. Site Description and Measurements

The Quistococha AmeriFlux site (PE-QFR; latitude −3.8344, longitude −73.3190; 104 m above sea level) is located near Iquitos, Peru (Griffis et al., 2020). Tree density and basal area are 1,846 ± 335 trees ha^{-1} and 19.4 ± 2.8 $m^2\ ha^{-1}$, respectively for stems with diameter at breast height greater than 10 cm (Bhomia et al., 2019). *Mauritia flexuosa* L.f. represents ∼65% of the total palm basal area (Bhomia et al., 2019).

Peat thickness is 1.92–2.45 m (Bhomia et al., 2019; Lähteenoja et al., 2009) with a total soil C pool of ∼740 Mg-C ha^{-1}. Total aboveground and belowground biomass C stocks are 97.7 ± 15 and 24.9 ± 4.1 Mg-C ha^{-1}, respectively (Bhomia et al., 2019). The mean annual air temperature and precipitation are 27.2°C and 2,753 mm, respectively (Griffis et al., 2020). The wetter and drier seasons typically occur during February–April and August–October, respectively. The water table position is often above the peat surface during the latter part of the wet season and rarely drops below a level of 20 cm from the peat surface (Hergoualc'h et al., 2020; Kelly et al., 2017).

Complete descriptions of the eddy covariance and hydrometeorological measurements are available in Text S1 in Supporting Information S1 and in Griffis et al. (2020). Eddy covariance data processing and gap-filling procedures (Burba et al., 2008; Deventer et al., 2019; Fratini et al., 2012; Horst & Lenschow, 2009; Moncrieff et al., 2005; Morgenstern et al., 2004; Papale et al., 2006; Tanner & Thurtell, 1969; Webb et al., 1980; J. D. Wood et al., 2017) are described in detail in Text S2 in Supporting Information S1. Briefly, observed net ecosystem CO_2 exchange was gap-filled following the marginal distribution sampling method implemented in REddyProc (Wutzler et al., 2018). The uncertainty in the annual totals resulting from data losses and gap-filling was determined using a Monte-Carlo approach (Griffis et al., 2003). Here, we report our first 3 complete full years of data: 2018, 2019, and 2022. The 2-year gap was caused by disruptions from lightning strikes and extended times to ship and repair equipment because of the Covid-19 pandemic. Owing to large gaps in rainfall measured at the tower, we used data from a weather station at Puerto Almendra, which is ∼6 km from the Quistococha site.

2.2. Data Analysis

We compared divergent ecosystem behavior across years by breaking the annual cycles down into 4 phases, which corresponded to DOY ranges of 1–45 (P1), 46–200 (P2), 201–300 (P3), and 301–365 (P4), respectively. The phases were defined based on when the behavior of the cumulative NEE curve for 2022 diverged from the curves for 2018 and 2019. We focused our analyses on NEE observations to avoid uncertainties associated with partitioning, which is challenging at this site because temperatures are stable at longer than sub-daily time scales. Note that at night, measured NEE corresponds to ecosystem respiration (R_{eco}) because there is no photosynthesis.

2.2.1. Flux and Meteorological Data

Flux and meteorological data were aggregated for each phase in each year, with 83% CIs computed taking autocorrelation into account (Zięba & Ramza, 2011). Presenting 83% CIs is a more appropriate visual aid for assessing statistical differences in means compared to the more common 95% CI (Goldstein & Healy, 1995). Means with non-overlapping 83% CIs can be interpreted as significantly different at $p < 0.05$ (Goldstein & Healy, 1995). We also conducted analysis of variance analyses to compare means within a phase using the approach of Lund et al. (2016), which was developed for cases with autocorrelated data (Text S3 in Supporting Information S1). Multiple means comparisons were conducted using Tukey's HSD and interpreted as significant if $p < 0.05$.

We report water table data as the "water table integral" (WTI) (Figure S5 in Supporting Information S1). This provides an integrated measure of the magnitude and duration that the water level is above (i.e., inundated) or below the surface. For each time period of interest, positive water table time was computed as $\text{WTI}_+ = \sum \max(\text{WT}_t, 0)$ and negative water table time was computed as $\text{WTI}_- = \sum \min(\text{WT}_t, 0)$, where WT_t is the 24-hr mean water table elevation. The total WTI is the sum of WTI_- and WTI_+.

2.2.2. Canopy Light Responses

For each phase of the three annual cycles, we fitted light response curves to enable comparison of canopy photosynthesis traits. Like our earlier work (Griffis et al., 2020), we fitted the rectangular hyperbolic light response to incoming photosynthetic photon flux density ($Q_\downarrow$):

$$-\text{NEE} = \frac{\phi_0 P_{\max} Q_\downarrow}{\phi_0 Q_\downarrow + P_{\max}} - R_d \tag{1}$$

where $P_{\max}$ is the maximal light-saturated canopy photosynthesis (i.e., gross primary productivity; μmol $\text{m}^{-2}\ \text{s}^{-1}$), ϕ_0 is the initial apparent quantum yield at $Q_\downarrow = 0$ μmol $\text{m}^{-2}\ \text{s}^{-1}$, and R_d is an estimate of daytime ecosystem respiration (μmol $\text{m}^{-2}\ \text{s}^{-1}$). For each phase, Equation 1 was fitted to all half hourly data for which $Q_\downarrow$ was >5 μmol $\text{m}^{-2}\ \text{s}^{-1}$ to retrieve $P_{\max}$, ϕ_0, and R_d (all free parameters) using MATLAB (R2022B, The MathWorks Inc., Natick MA) using the `lsqcurvefit.m` function. The Jacobian matrix of the solution was used to estimate 83% CIs using the `nlparci.m` function. Following de A. Lobo et al. (2013), we used the fitted light response parameters to calculate the light compensation point (LCP), as well as quantum yields at the LCP (ϕ_{LCP}) and at $Q_\downarrow = 300$ μmol $\text{m}^{-2}\ \text{s}^{-1}$, ϕ_{300} (Text S4 in Supporting Information S1).

2.3. Evaluation of Hypotheses

We evaluated hypotheses by comparing fluxes and hydrometeorology across phases of the annual cycle across years and analyzing canopy light responses. The tests were designed to diagnose the mechanisms underlying the shift in the net CO_2 budget from strong sink (2018/2019) to C neutrality (2022) and were evaluated for each phase of the annual cycle.

The *Respiration Hypothesis* was evaluated by testing for amplified ecosystem respiration coincident with water tables below the surface, a classic peatland response associated with increased heterotrophic respiration in oxic peat layers (Hirano et al., 2012; Kiew et al., 2018). Indeed, Ma et al. (2022) found a globally robust relationship between declining water tables and increasing CO_2 emissions from peatlands. We assume that higher R_{eco} during periods with water tables below the surface is largely driven by increases in soil respiration rather than autotrophic respiration, which was noted by Ma et al. (2022).

The *Photoinhibition Hypothesis* was evaluated by testing for changes in light response parameters (Figure S1 in Supporting Information S1) as conceptualized in Murchie and Niyogi (2011). Moderate photoinhibition is characterized by (a) decreased quantum yields at sub-saturating light, (b) increased LCP, and (c) no change in $P_{\max}$. Severe photoinhibition would show further (a) decreased quantum yields, and (b) increased LCP, with (c) decreased $P_{\max}$. In the case of moderate photoinhibition, the lower quantum yields at low light decreases CO_2 assimilation during these times, while under full midday sun CO_2 uptake would remain high. Because photosynthesis exhibits many environmental responses it can be difficult to disentangle mechanisms causing declines in CO_2 assimilation (Busch et al., 2024; Murchie & Niyogi, 2011). We therefore test for the changes in light response parameters that occur during periods with higher-than-normal light, but without marked differences in other environmental variables.

3. Results

Across the 2018 and 2019 annual cycles, cumulative NEE did not deviate beyond the limits of uncertainties, with annual fluxes of −466 [−564.8, −380.0] and −461 [−531.7, −400.9] g-C m^{-2} y^{-1}, respectively (Figure 1a). In contrast, cumulative NEE in 2022 was consistently higher (i.e., less negative) across the annual cycle, ending the year at 20 [−47.9, 88.3] g-C m^{-2} y^{-1}. Early in 2022 (P1) the forest was CO_2 neutral, while the other years were strong CO_2 sinks. Eventually in 2022 (P2), the forest became a consistent, but smaller CO_2 sink compared to the other years. In all years, the forest behaved as a CO_2 source for an extended period during P3 (roughly corresponding to the drier season), but the highest emissions occurred in 2022 when the water table drawdown was the strongest in the record (Figure 2i). At the end of 2022 (P4), the forest returned to CO_2 neutral behavior while the other years were CO_2 sinks.

The hydrometeorology during 2022 showed several notable deviations compared to 2018 and 2019, with significantly higher daily light integrals (DLI) and daily maximum $Q_{\downarrow}$ at the beginning and the end of the year, that is, P1 and P4, respectively (Figures 2a and 2d). There was also less rainfall during these phases of 2022, though the difference was only notable at the end of the year (Figure 2g and Table S2 in Supporting Information S1), while VPD equaled or was significantly higher than the other years (Figure 2c). Air temperatures were, however, more consistent among years (Figures 2b, 2e, and 2h). Importantly, water table dynamics stood out in 2022, with P3 having the largest drawdown and most sustained period with water tables below the surface, while water table elevations were generally higher throughout the rest of the year (Figure 2i, Figure S3 and Table S3 in Supporting Information S1).

3.1. Phases 1 and 4: Beginnings and Endings of the Annual Cycles

Early in the strong sink years, nighttime R_{eco} and daytime NEE deviated from one another (Figures 1b and 1c, respectively), while the nighttime R_{eco} to daytime NEE ratios (Figure S2 in Supporting Information S1) and thus cumulative NEE were consistent (Figure 1a). The overall ecosystem metabolism was thus scaled down in 2019 compared to 2018. Indeed, the start of 2019 stood out as having the lowest $P_{\max}$, R_d as well as lowest $Q_{\downarrow}$ relative to the other years at the same time (Figures 3c, 3e, 2a, and 2d, respectively). During early 2022, nighttime R_{eco} was consistent with one of the strong sink years (2018), with both being higher than 2019. Additionally, none of the years displayed a strong water table drawdown (Figure 2i, Figure S3 and Table S3 in Supporting Information S1). Taken together, these observations are not consistent with the Respiration Hypothesis. Daytime NEE was the lowest in 2022, though not significantly different from 2019 ($p = 0.067$), implying that canopy photosynthesis may have been impaired.

When the forest was CO_2 neutral during early and late 2022 (Figure 1a), the LCP was significantly higher, while ϕ_0 and ϕ_{300} (i.e., light-use efficiency at different light levels) were lower compared to the strong sink years (Figures 3a, 3b, and 3f, respectively). Notably, R_d did not show enhancement relative to both other years (Figure 3e), supporting that canopy photosynthesis was suppressed during P1 and P4 of 2022. The absence of (a) strong R_{eco} enhancement during nighttime or daytime (i.e., R_{d}) and (b) strong water table drawdowns (Figure 2i, Figure S3 and Table S3 in Supporting Information S1) during these phases of 2022 versus the other years supports the hypothesis that the smaller CO_2 sink was a symptom of inhibition of canopy photosynthesis rather than a heterotrophic respiration response.

Early and late 2022 were characterized by unusually high light and/or VPD (Figures 2a, 2c, and 2d). Across all phases and years, the quantum yields (ϕ_0, ϕ_{LCP}, and ϕ_{300}) were significantly anticorrelated with mean DLI, while

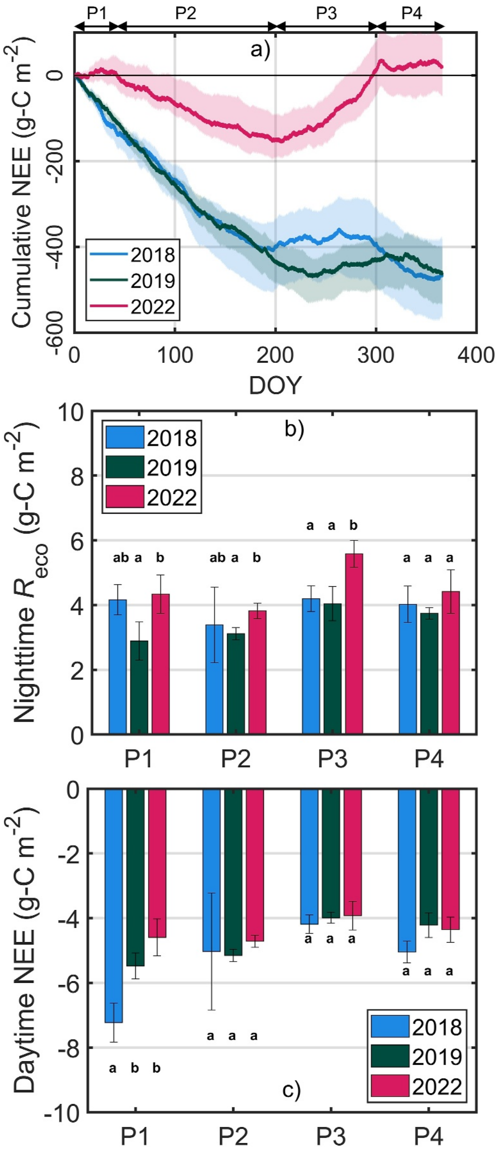

Figure 1. (a) Cumulative (calculated as the running sum) net ecosystem CO_2 exchange (NEE) of an Amazonian palm swamp peatland; shaded areas represent uncertainties of cumulative flux integrals; and the mean (±83% confidence intervals) of (b) nighttime ecosystem respiration (R_{eco}), and (c) daytime NEE for the different phases of the annual cycles. Within phases, means sharing the same letter are not significantly different ($p < 0.05$).

the LCP was significantly correlated with mean DLI (Figure S4 in Supporting Information S1), which are responses consistent with moderate photoinhibition of photosynthesis (Murchie & Niyogi, 2011). The LCP was also significantly correlated with daytime VPD. In contrast, $P_{\max}$ was correlated with neither light nor VPD. These results demonstrate that exposure to more stressful conditions of high light and/or VPD compromises LUE and decreases CO_2 assimilation at low light.

The lack of atypically high respiration during nighttime or daytime (Figures 1b and 3e, respectively), combined with the unusually low canopy quantum yields and high LCP supports the Photoinhibition of Photosynthesis Hypothesis and that impaired canopy photosynthesis during early and late 2022 drove the net CO_2 neutral behavior (Figure 1a).

3.2. Phase 2: Usually a Strong CO_2 Sink

Unlike the other phases, the hydrometeorology during P2 of 2022 did not present anomalies consistent with our hypotheses. Though mean daily maximum $Q_{\downarrow}$ was significantly higher than the other years, this was not the case for the DLI (Figures 2d and 2a, respectively), which represents integrated exposure to light. However, water table elevations were the highest during 2022, though the peatland was usually flooded for most of this phase of the annual cycle.

During P2, the forest was a net CO_2 sink in 2022, though it was weaker than the other years (Figure 1a), which may have been caused by sustained LUE disadvantage at low light as evidenced by significantly lower ϕ_0, ϕ_{LCP}, and ϕ_{300} relative to the other years based on comparing the estimates and their 83% CIs (Figures 3b, 3d, and 3f). While there were differences in quantum yields, they were not as striking as was the case in P1. It is notable that we did not find a striking difference in LCP as was the case for P1 (Figure 3a). The forest was thus able to recover photosynthetic function during this cooler phase in 2022 (Figures 2b, 2e, and 2h).

Once the peat is completely flooded and anoxic, higher water tables are unlikely to substantially alter biogeochemical cycling and heterotrophic respiration. It is, however, possible that autotrophic respiration could be suppressed if trees become stressed. The respiration data do not offer compelling evidence to make any judgment in this regard. In 2022, R_d was consistent with 2019 or substantially lower than 2018 (Figure 3e). Furthermore, nighttime R_{eco} was highest in 2022, though only significantly higher than 2019 (Figure 1b), while daytime NEE was consistent across years (Figure 1c).

These results demonstrate that in 2022, there was probably some residual damage that was incurred by exposure to high light during P1 (evidenced by the lower quantum yields). However, mean daytime NEE was similar across years (Figure 1c), so if there was photoinhibition, it was not strong enough to leave a clear imprint on the carbon balance. Additionally, nighttime R_{eco} did not display anomalous behavior consistent with the Respiration Hypothesis. We thus reject both the Respiration and Photoinhibition hypotheses. It is thus likely that there were subtle differences in ecosystem functioning too small to detect that gave rise to the lower sink strength.

3.3. Phase 3: Usually a Small CO_2 Source

During the drier season (P3), the forest had been a small source or close to CO_2 neutral in 2018 and 2019 (Figure 1a). However, in 2022, mean nighttime R_{eco} was the highest observed over the 3 years (Figure 1b) while daytime net CO_2 uptake was consistent with the strong sink years (Figure 1c), giving a ratio of nighttime R_{eco} to daytime NEE of ~1.4 that was the highest on record (Figure S2 in Supporting Information S1). Furthermore, the

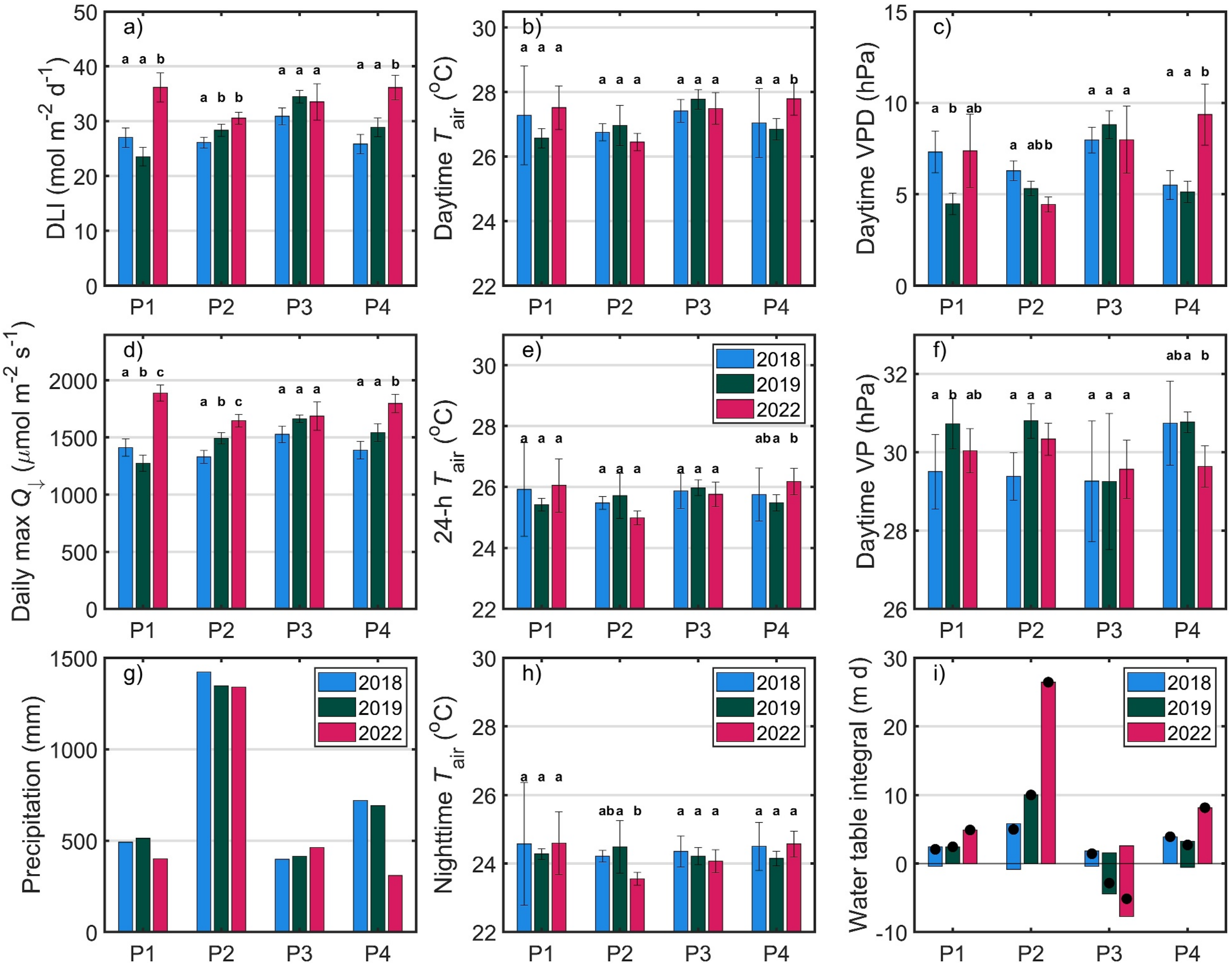

Figure 2. Meteorological variability over the four phases of the annual cycles (a–i). Bars represent the mean (±83% confidence interval). In panel (i) the positive and negative integrated water table integrals are shown as bars, and the total water table integral as the black circles. Within phases, means sharing the same letter are not significantly different ($p < 0.05$). DLI, daily light integral; $Q_\downarrow$, incident photosynthetic photon flux density; VP, vapor pressure; VPD, vapor pressure deficit; and T_{air}, air temperature.

lowest water tables, which were consistently below the surface, were also observed during this phase of 2022 (Figure 2i, Figure S3 and Table S3 in Supporting Information S1). There was no compelling evidence supporting photoinhibition of canopy photosynthesis.

These observations support the Respiration Hypothesis and that an amplified heterotrophic respiration signal was responsible for the strong net CO_2 source behavior in P3 of 2022 (Figure 1a).

4. Discussion and Conclusions

Soil C accumulation at this site has averaged 74 ± 15 g-C m^{-2} y^{-1} over the last 2,300 years (Lähteenoja et al., 2009) indicating consistent C sink behavior. Our early eddy covariance measurements suggested a recent sink strength of ~450 g-C m^{-2} y^{-1} (Griffis et al., 2020). Modeling studies suggest that under an extreme scenario, the C sink of Amazonian peatlands is vulnerable to warming toward the end of the 21st century (Wang et al., 2018). Our finding that the site switched from a strong C sink to carbon under contemporary environmental variation was thus surprising.

Our results support both the Respiration and Photoinhibition of Photosynthesis Hypotheses as explanations for the C neutral behavior of the forested peatland during 2022. At certain times, there was evidence supporting both hypotheses; however, these mechanisms were active at different times.

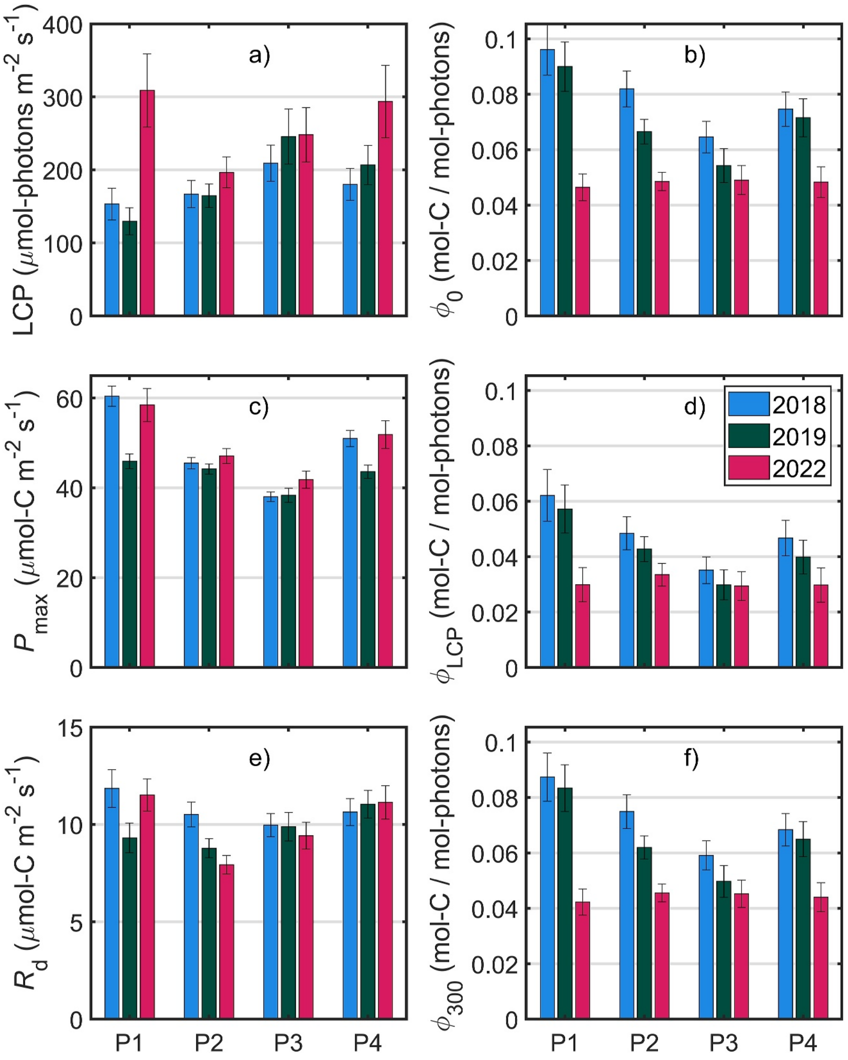

Figure 3. Variations of canopy light response parameters (error bars indicate 83% confidence intervals) during phases of the annual cycles (a–f). LCP, apparent canopy light compensation point; P_{max}, maximal gross canopy photosynthesis; R_d, daytime respiration; ϕ_0, apparent canopy quantum yield at zero light; ϕ_{LCP}, apparent canopy quantum yield at the LCP; and ϕ_{300}, apparent canopy quantum yield at light = 300 μmol m^{-2} s^{-1}.

When water tables fall below the surface peat layers are exposed to oxic conditions, which increases soil respiration rates (Hirano et al., 2012; Kiew et al., 2018; Ma et al., 2022). We found clear evidence of this behavior, supporting the *Respiration Hypothesis* during the drier season (P3) of 2022 when the forest was the strongest net CO_2 source of the 3 years (Figure 1a), and there was the strongest water table drawdown and highest nighttime R_{eco} (Figures 2i and 1b, respectively), the latter being 33%–38% higher than the other years.

During early and late 2022, we noted important changes in canopy light responses that point to decreased LUE, particularly during periods of low light (Figures 3a, 3b, 3d, and 3f), while P_{max} was unaffected (Figure 3c). During these times, DLIs were 25%–54% higher than the other years at the same times (Figure 2a). Furthermore, DLIs were above 30 mol m^{-2} d^{-1} across the whole 2022 annual cycle, while in the other years this was the case only during the drier season (P3, DOY 201–300). We hypothesize that the considerably brighter conditions contributed to moderate photoinhibition of photosynthesis, which decreased the magnitude of the CO_2 sink.

Under high light, excitation energy exceeds capacity for electron transport (Gu et al., 2019). Managing the excess energy is an essential function facilitated through nonphotochemical quenching, which represents a collection of processes (Kramer et al., 2004; Murchie & Niyogi, 2011; Papageorgiou & Govindjee, 2004). From a photoprotection standpoint, energy-dependent quenching (qE) occurs on timescales of seconds to minutes and is most important, dissipating much of the excitation energy as heat (Gu et al., 2019; Murchie & Niyogi, 2011). If light intensity is sustained above saturation for long periods of time, quenching by photoinhibition (qI) occurs, whereby photosystem II (PSII) is subject to irreversible inactivation from which recovery requires protein synthesis in chloroplasts (Tyystjärvi, 2013; Yamamoto et al., 2013). Photoinhibition can be moderate or severe, whereby quantum yields decrease without or with a reduction in maximal photosynthetic CO_2 uptake (Murchie & Niyogi, 2011).

Our light response analyses were consistent with moderate photoinhibition influencing canopy quantum yields without compromising $P_{\max}$. This was most notable during early and late 2022, when light was significantly higher than other years. It is also noteworthy that during these times, VPD was high, either matching at least one of the other years or significantly exceeding by 65%–83% (Figure 2c). The high radiation loads and VPD reflect high atmospheric demand for water vapor. If the vascular system of the plants cannot deliver enough water to match atmospheric demand, leaves can dehydrate and lose turgor (Sack & Holbrook, 2006)—even when growing in a (temperate) bog with plentiful water in the peat profile (Warren et al., 2021). Photoinhibition may be compounded by other stresses like water deficits that influence PSII structure and function (Hu et al., 2023). We do not have direct observations of leaf water potentials, so we can only speculate that the higher atmospheric demand could have led to compounding stresses that exacerbated photoinhibition. Our results suggest that outside of the drier season, the forest is sensitive to photoinhibition when there are sustained periods with $Q_{\downarrow} > 30$ mol m^{-2} d^{-1}. Future studies of canopy sun-induced fluorescence to probe the light reactions of photosynthesis (Gu et al., 2019, 2023; Sun, Gu, et al., 2023; Sun, Wen, et al., 2023), and more specifically, changes in energy partitioning in the photosystems will develop deeper understanding of the susceptibility of these systems to photoinhibition.

Historically, peatland carbon cycling has been viewed through the lens of how disturbances or environmental change impact water table dynamics, and how the aeration of peat releases CO_2 (Hirano et al., 2012; Kiew et al., 2018; Ma et al., 2022). Warming and declining water tables can shift peatlands from C sink to source (Hanson et al., 2020), and projections indicate climate change may cause this shift in Amazonian peatlands (Wang et al., 2018). Our results add to the body of evidence that peatlands in general, and specifically in the Amazon, are at risk of losing large quantities of carbon when water tables fall below the surface. Additionally, we find novel evidence that Amazonian peatland forests are subject to photoinhibition of photosynthesis during clear weather.

Recent studies of the photosynthetic responses of Amazonian forests have focused on how VPD (Green et al., 2020) or soil moisture (Green et al., 2019) influence plant water relations and thus stomatal conductance. Our findings suggest that tropical rainforests could be more sensitive to photoinhibition than previously thought. Photoinhibition has been recognized in the tropics, particularly in humid seasonally dry areas (Krause & Winter 2021), with particular concern for the ecology of shade-grown understory plants after a disturbance (Lovelock et al., 1994), but not at canopy scale. Further investigations are warranted to determine if canopy photoinhibition is generalizable, and if so, how to address it within a modeling framework.

Our results show that the CO_2 budgets of peatland forests in the Peruvian Amazon are sensitive to fluctuations in both water table and changes in the light environment. Our findings imply that these forests are sensitive to photoinhibition during key parts of the annual cycle, notably transitional between the drier and wetter seasons (i.e., P1 and P4). Further efforts to characterize leaf water relations and photosynthetic traits in these forests will help to better understand and predict how vulnerable these systems are to changes in light environment.

Conflict of Interest

The authors declare no conflicts of interest relevant to this study.

Data Availability Statement

The half-hourly flux and hydrometeorological data forming the basis of analyses reported in this manuscript are available from AmeriFlux (site ID: PE-QFR). The aggregated flux and hydrometeorological data used for analyses in this paper are available from ESS-DIVE (J. Wood et al., 2025).

Acknowledgments

This material is based upon work supported by the U.S. Department of Energy, Office of Science, Office of Biological and Environmental Research, Terrestrial Ecosystem Science Program, under Award DE-SC0020167.

References

Bhomia, R. K., van Lent, J., Rios, J. M. G., Hergoualc'h, K., Coronado, E. N. H., & Murdiyarso, D. (2019). Impacts of Mauritia flexuosa degradation on the carbon stocks of freshwater peatlands in the Pastaza-Marañón river basin of the Peruvian Amazon. *Mitigation and Adaptation Strategies for Global Change*, *24*(4), 645–668. https://doi.org/10.1007/s11027-018-9809-9

Burba, G. G., McDermitt, D. K., Grelle, A., Anderson, D. J., & Xu, L. (2008). Addressing the influence of instrument surface heat exchange on the measurements of CO_2 flux from open-path gas analyzers. *Global Change Biology*, *14*(8), 1854–1876. https://doi.org/10.1111/j.1365-2486.2008.01606.x

Busch, F. A., Ainsworth, E. A., Amtmann, A., Cavanagh, A. P., Driever, S. M., Ferguson, J. N., et al. (2024). A guide to photosynthetic gas exchange measurements: Fundamental principles, best practice and potential pitfalls. *Plant, Cell and Environment*, *47*(9), 3344–3364. https://doi.org/10.1111/pce.14815

de A. Lobo, F., de Barros, M. P., Dalmagro, H. J., Dalmolin, Â. C., Pereira, W. E., de Souza, É. C., et al. (2013). Fitting net photosynthetic light-response curves with Microsoft Excel - A critical look at the models. *Photosynthetica*, *51*(3), 445–456. https://doi.org/10.1007/s11099-013-0045-y

Deshmukh, C. S., Julius, D., Desai, A. R., Asyhari, A., Page, S. E., Nardi, N., et al. (2021). Conservation slows down emission increase from a tropical peatland in Indonesia. *Nature Geoscience*, *14*(7), 484–490. https://doi.org/10.1038/s41561-021-00785-2

Deventer, M. J., Griffis, T. J., Roman, D. T., Kolka, R. K., Wood, J. D., Erickson, M., et al. (2019). Error characterization of methane fluxes and budgets derived from a long-term comparison of open- and closed-path eddy covariance systems. *Agricultural and Forest Meteorology*, *278*, 107638. https://doi.org/10.1016/j.agrformet.2019.107638

Fratini, G., Ibrom, A., Arriga, N., Burba, G., & Papale, D. (2012). Relative humidity effects on water vapour fluxes measured with closed-path eddy-covariance systems with short sampling lines. *Agricultural and Forest Meteorology*, *165*, 53–63. https://doi.org/10.1016/j.agrformet.2012.05.018

Goldstein, H., & Healy, M. J. R. (1995). The graphical presentation of a collection of means. *Journal of the Royal Statistical Society: Series A*, *158*(1), 175–177. https://doi.org/10.2307/2983411

Green, J. K., Berry, J., Ciais, P., Zhang, Y., & Gentine, P. (2020). Amazon rainforest photosynthesis increases in response to atmospheric dryness. *Science Advances*, *6*(47), 1–9. https://doi.org/10.1126/sciadv.abb7232

Green, J. K., Seneviratne, S. I., Berg, A. M., Findell, K. L., Hagemann, S., Lawrence, D. M., & Gentine, P. (2019). Large influence of soil moisture on long-term terrestrial carbon uptake. *Nature*, *565*(7740), 476–479. https://doi.org/10.1038/s41586-018-0848-x

Griffis, T. J., Black, T. A., Morgenstern, K., Barr, A. G., Nesic, Z., Drewitt, G. B., et al. (2003). Ecophysiological controls on the carbon balances of three southern boreal forests. *Agricultural and Forest Meteorology*, *117*(1–2), 53–71. https://doi.org/10.1016/S0168-1923(03)00023-6

Griffis, T. J., Roman, D. T., Wood, J. D., Deventer, J., Fachin, L., Rengifo, J., et al. (2020). Hydrometeorological sensitivities of net ecosystem carbon dioxide and methane exchange of an Amazonian palm swamp peatland. *Agricultural and Forest Meteorology*, *295*, 108167. https://doi.org/10.1016/j.agrformet.2020.108167

Gu, L., Grodzinski, B., Han, J., Marie, T., Zhang, Y. J., Song, Y. C., & Sun, Y. (2023). An exploratory steady-state redox model of photosynthetic linear electron transport for use in complete modelling of photosynthesis for broad applications. *Plant, Cell and Environment*, *46*(5), 1540–1561. https://doi.org/10.1111/pce.14563

Gu, L., Han, J., Wood, J. D., Chang, C. Y. Y., & Sun, Y. (2019). Sun-induced Chl fluorescence and its importance for biophysical modeling of photosynthesis based on light reactions. *New Phytologist*, *223*(3), 1179–1191. https://doi.org/10.1111/nph.15796

Hanson, P. J., Griffiths, N. A., Iversen, C. M., Norby, R. J., Sebestyen, S. D., Phillips, J. R., et al. (2020). Rapid net carbon loss from a whole-ecosystem warmed peatland. *AGU Advances*, *1*(3), e2020AV000163. https://doi.org/10.1029/2020av000163

Hastie, A., Honorio Coronado, E. N., Reyna, J., Mitchard, E. T. A., Åkesson, C. M., Baker, T. R., et al. (2022). Risks to carbon storage from land-use change revealed by peat thickness maps of Peru. *Nature Geoscience*, *15*(5), 369–374. https://doi.org/10.1038/s41561-022-00923-4

Hastie, A., Householder, J. E., Honorio Coronado, E. N., Hidalgo Pizango, C. G., Herrera, R., Lähteenoja, O., et al. (2024). A new data-driven map predicts substantial undocumented peatland areas in Amazonia. *Environmental Research Letters*, *19*(9), 094019. https://doi.org/10.1088/1748-9326/ad677b

Hergoualc'h, K., Dezzeo, N., Verchot, L. V., Martius, C., van Lent, J., del Aguila-Pasquel, J., & López Gonzales, M. (2020). Spatial and temporal variability of soil N_2O and CH_4 fluxes along a degradation gradient in a palm swamp peat forest in the Peruvian Amazon. *Global Change Biology*, *26*(12), 7198–7216. https://doi.org/10.1111/gcb.15354

Hirano, T., Segah, H., Harada, T., Limin, S., June, T., Hirata, R., & Osaki, M. (2007). Carbon dioxide balance of a tropical peat swamp forest in Kalimantan, Indonesia. *Global Change Biology*, *13*(2), 412–425. https://doi.org/10.1111/j.1365-2486.2006.01301.x

Hirano, T., Segah, H., Kusin, K., Limin, S., Takahashi, H., & Osaki, M. (2012). Effects of disturbances on the carbon balance of tropical peat swamp forests. *Global Change Biology*, *18*(11), 3410–3422. https://doi.org/10.1111/j.1365-2486.2012.02793.x

Horst, T. W., & Lenschow, D. H. (2009). Attenuation of scalar fluxes measured with spatially-displaced sensors. *Boundary-Layer Meteorology*, *130*(2), 275–300. https://doi.org/10.1007/s10546-008-9348-0

Hu, C., Elias, E., Nawrocki, W. J., & Croce, R. (2023). Drought affects both photosystems in Arabidopsis thaliana. *New Phytologist*, *240*(2), 663–675. https://doi.org/10.1111/nph.19171

Kelly, T. J., Lawson, I. T., Roucoux, K. H., Baker, T. R., Jones, T. D., & Sanderson, N. K. (2017). The vegetation history of an Amazonian domed peatland. *Palaeogeography, Palaeoclimatology, Palaeoecology*, *468*, 129–141. https://doi.org/10.1016/j.palaeo.2016.11.039

Kiew, F., Hirata, R., Hirano, T., Wong, G. X., Aeries, E. B., Musin, K. K., et al. (2018). CO_2 balance of a secondary tropical peat swamp forest in Sarawak, Malaysia. *Agricultural and Forest Meteorology*, *248*, 494–501. https://doi.org/10.1016/j.agrformet.2017.10.022

Kiew, F., Hirata, R., Hirano, T., Xhuan, W. G., Aries, E. B., Kemudang, K., et al. (2020). Carbon dioxide balance of an oil palm plantation established on tropical peat. *Agricultural and Forest Meteorology*, *295*, 108189. https://doi.org/10.1016/j.agrformet.2020.108189

Kramer, D. M., Johnson, G., Kiirats, O., & Edwards, G. E. (2004). New fluorescence parameters for the determination of Q_A redox state and excitation energy fluxes. *Photosynthesis Research*, *79*(2), 209–218. https://doi.org/10.1023/B:PRES.0000015391.99477.0d

Krause, G. H., & Winter, K. (2021). The photosynthetic system in tropical plants under high irradiance and temperature stress. In F. M. Cánovas, U. Lüttge, M.-C. Risueño, & H. Pretzsch (Eds.), *Progress in botany* (Vol. 82, pp. 131–169). Springer. https://doi.org/10.1007/124_2020_44

Lähteenoja, O., Ruokolainen, K., Schulman, L., & Oinonen, M. (2009). Amazonian peatlands: An ignored C sink and potential source. *Global Change Biology*, *15*(9), 2311–2320. https://doi.org/10.1111/j.1365-2486.2009.01920.x

López Gonzales, M., Hergoualc'h, K., Angulo Núñez, Ó., Baker, T., Chimner, R., del Águila Pasquel, J., et al. (2020). *What do we know about Peruvian peatlands? Occasional paper 210*. CIFOR. https://doi.org/10.17528/cifor/007848

Lovelock, C. E., Osmond, C. B., & Jebb, M. (1994). Photoinhibition and recovery in tropical plant species: Response to disturbance. *Oecologia*, *97*(3), 297–307. https://doi.org/10.1007/BF00317318

Lund, R., Liu, G., & Shao, Q. (2016). A new approach to ANOVA methods for autocorrelated data. *The American Statistician*, *70*(1), 55–62. https://doi.org/10.1080/00031305.2015.1093026

Ma, L., Zhu, G., Chen, B., Zhang, K., Niu, S., Wang, J., et al. (2022). A globally robust relationship between water table decline, subsidence rate, and carbon release from peatlands. *Communications Earth & Environment*, *3*(1), 254. https://doi.org/10.1038/s43247-022-00590-8

Moncrieff, J., Clement, R., Finnigan, J., & Meyers, T. (2005). Averaging, detrending, and filtering of eddy covariance time series. In X. Lee, W. Massman, & B. Law (Eds.), *Handbook of Micrometeorology: A Guide for Surface Flux Measurement and Analysis* (pp. 7–31). Springer. https://doi.org/10.1007/1-4020-2265-4_2

Morgenstern, K., Black, T. A., Humphreys, E. R., Griffis, T. J., Drewitt, G. B., Cai, T., et al. (2004). Sensitivity and uncertainty of the carbon balance of a Pacific Northwest Douglas-fir forest during an El Niño/La Niña cycle. *Agricultural and Forest Meteorology*, *123*(3–4), 201–219. https://doi.org/10.1016/j.agrformet.2003.12.003

Murchie, E. H., & Niyogi, K. K. (2011). Manipulation of photoprotection to improve plant photosynthesis. *Plant Physiology*, *155*(1), 86–92. https://doi.org/10.1104/pp.110.168831

Ohkubo, S., Hirano, T., & Kusin, K. (2021). Assessing the carbon dioxide balance of a degraded tropical peat swamp forest following multiple fire events of different intensities. *Agricultural and Forest Meteorology*, *306*, 108448. https://doi.org/10.1016/j.agrformet.2021.108448

Papageorgiou, G. C., & Govindjee, G. (2004). Chlorophyll a fluorescence: A signature of photosynthesis. In G. C. Papageorgiou & G. Govindjee (Eds.), *Advances in photosynthesis and respiration* (Vol. 19). Springer. https://doi.org/10.1016/S0005-2728(99)00047-X

Papale, D., Reichstein, M., Aubinet, M., Canfora, E., Bernhofer, C., Kutsch, W., et al. (2006). Towards a standardized processing of Net Ecosystem Exchange measured with eddy covariance technique: Algorithms and uncertainty estimation. *Biogeosciences*, *3*(4), 571–583. https://doi.org/10.5194/bg-3-571-2006

Ribeiro, K., Pacheco, F. S., Ferreira, J. W., de Sousa-Neto, E. R., Hastie, A., Krieger Filho, G. C., et al. (2020). Tropical peatlands and their contribution to the global carbon cycle and climate change. *Global Change Biology*, *27*(3), 489–505. https://doi.org/10.1111/gcb.15408

Sack, L., & Holbrook, N. M. (2006). Leaf hydraulics. *Annual Review of Plant Biology*, *57*(1), 361–381. https://doi.org/10.1146/annurev.arplant.56.032604.144141

Sun, Y., Gu, L., Wen, J., van der Tol, C., Porcar-Castell, A., Joiner, J., et al. (2023). From remotely sensed solar-induced chlorophyll fluorescence to ecosystem structure, function, and service: Part I—Harnessing theory. *Global Change Biology*, *29*(11), 2926–2952. https://doi.org/10.1111/gcb.16634

Sun, Y., Wen, J., Gu, L., Joiner, J., Chang, C. Y., van der Tol, C., et al. (2023). From remotely-sensed solar-induced chlorophyll fluorescence to ecosystem structure, function, and service: Part II—Harnessing data. *Global Change Biology*, *29*(11), 2893–2925. https://doi.org/10.1111/gcb.16646

Tang, A. C. I., Melling, L., Stoy, P. C., Musin, K. K., Aeries, E. B., Waili, J. W., et al. (2020). A Bornean peat swamp forest is a net source of carbon dioxide to the atmosphere. *Global Change Biology*, *26*(12), 6931–6944. https://doi.org/10.1111/gcb.15332

Tanner, C. B., & Thurtell, G. W. (1969). *Anemoclinometer measurements of Reynolds stress and heat transport in the atmospheric surface layer*. Research and Development Technical Report, ECOM 66-G22-F.

Tyystjärvi, E. (2013). Photoinhibition of photosystem II. In *International review of cell and molecular biology* (Vol. 300). https://doi.org/10.1016/B978-0-12-405210-9.00007-2

UNEP. (2022). *Global peatlands assessment – The State of the World's Peatlands: Evidence for action toward the conservation, restoration, and sustainable management of peatlands*. Main Report. United Nations Environment Programme.

Wang, S., Zhuang, Q., Lähteenoja, O., Draper, F. C., & Cadillo-Quiroz, H. (2018). Potential shift from a carbon sink to a source in Amazonian peatlands under a changing climate. *Proceedings of the National Academy of Sciences of the United States of America*, *115*(49), 12407–12412. https://doi.org/10.1073/pnas.1801317115

Warren, J. M., Jensen, A. M., Ward, E. J., Guha, A., Childs, J., Wullschleger, S. D., & Hanson, P. J. (2021). Divergent species-specific impacts of whole ecosystem warming and elevated CO_2 on vegetation water relations in an ombrotrophic peatland. *Global Change Biology*, *27*(9), 1820–1835. https://doi.org/10.1111/gcb.15543

Webb, E. K., Pearman, G. I., & Leuning, R. (1980). Correction of flux measurements for density effects due to heat and water vapour transfer. *Quarterly Journal of the Royal Meteorological Society*, *106*(447), 85–100. https://doi.org/http://dx.doi.org/10.1002/qj.49710644707

Wood, J. D., Griffis, T. J., Baker, J. M., Frankenberg, C., Verma, M., & Yuen, K. (2017). Multiscale analyses of solar-induce fluorescence and gross primary production. *Geophysical Research Letters*, *44*, 533–541. https://doi.org/10.1002/2016GL070775

Wood, J., Roman, T., Rengifo, J., & Griffis, T. (2025). Aggregated carbon dioxide flux and hydrometeorology data from an Amazonian palm swamp peatland in Peru: 2018, 2019, and 2022 [Dataset]. *Biophysical processes and Feedback Mechanisms Controlling the Methane Budget of an Amazonian Peatland*. https://doi.org/10.15485/2565224

Wutzler, T., Lucas-Moffat, A., Migliavacca, M., Knauer, J., Sickel, K., Šigut, L., et al. (2018). Basic and extensible post-processing of eddy covariance flux data with REddyProc. *Biogeosciences*, *15*(16), 5015–5030. https://doi.org/10.5194/bg-15-5015-2018

Yamamoto, Y., Hori, H., Kai, S., Ishikawa, T., Ohnishi, A., Tsumura, N., & Morita, N. (2013). Quality control of photosystem II: Reversible and irreversible protein aggregation decides the fate of photosystem II under excessive illumination. *Frontiers in Plant Science*, *4*, 443. https://doi.org/10.3389/fpls.2013.00433

Yu, Z. C. (2012). Northern peatland carbon stocks and dynamics: A review. *Biogeosciences*, *9*(10), 4071–4085. https://doi.org/10.5194/bg-9-4071-2012

Yu, Z., Beilman, D. W., Frolking, S., MacDonald, G. M., Roulet, N. T., Camill, P., & Charman, D. J. (2011). Peatlands and their role in the global carbon cycle. *Eos, Transactions, American Geophysical Union*, *92*(12), 97–108. https://doi.org/10.1029/2012EO030008

Zięba, A., & Ramza, P. (2011). Standard deviation of the mean of autocorrelated observations estimated with the use of the autocorrelation function estimated from the data. *Metrology and Measurement Systems*, *18*(4), 529–542. https://doi.org/10.2478/v10178-011-0052-x